

# Matrix-Isolation FT-IR Studies and *ab Initio* Calculations of Hydrogen-Bonded Complexes of Molecules Modeling Cytosine or Isocytosine Tautomers. 6. Experimental Observation of a Water-Induced Tautomeric Shift for 2-Hydroxypyrimidine and 5-Bromo-2-hydroxypyrimidine

Johan Smets,<sup>†</sup> Alain Destexhe,<sup>†</sup> Ludwik Adamowicz,<sup>\*,‡</sup> and Guido Maes<sup>\*,†,§</sup>

Department of Chemistry, University of Leuven, Celestijnenlaan 200F, B-3001, Heverlee, Belgium, and  
Department of Chemistry, University of Arizona, Tucson, Arizona 85721

Received: April 10, 1998

The H-bond interaction of the cytosine model compound 2-hydroxypyrimidine and its 5-bromo derivative with water is investigated using the combined matrix-isolation FT-IR and theoretical *ab initio* method. As predicted by the *ab initio* calculations, both compounds occur dominantly in the hydroxy tautomeric forms. The estimated  $K_T(h/o)$  values are 60 and 184, respectively. When water is added to the Ar matrix, a noticeable shift of the tautomeric equilibrium towards the oxo form is observed. The theoretical results indicate that the closed  $N\cdots H-O(H)\cdots H-O$  and  $C=O\cdots H-O(H)\cdots H-N$  H-bonded water complexes are the most stable systems for the hydroxy and the oxo tautomers, respectively. The experimental spectra are consistent with this prediction, but additional structures, such as an open  $N\cdots H-OH$  complex of the hydroxy tautomer, are also identified. The frequency shift of the stretching mode of doubly H-bonded water in the two closed complexes is larger, and the ratio between the calculated and measured frequencies smaller than expected from the correlation established before for open, singly H-bonded complexes involving similar molecules. Although some cooperativity exists between the two H bonds in each of the closed complexes, this effect is limited because the geometrical structures of both H bonds are noticeably perturbed from the perfect alignment due to the cyclic arrangement of the complex. A possible mechanism of the proton transfer process leading from the hydroxy to the oxo tautomeric form is discussed in terms of proton tunneling and in relation to recent literature data.

## Introduction

In the former papers of this series, hydrogen bonding of the cytosine model molecules pyridine/pyrimidine,<sup>1</sup> 4-aminopyridine/4-aminopyrimidine,<sup>2</sup> 3-hydroxypyridine/4-hydroxypyridine,<sup>3</sup> 1-methyl-2-pyrimidone, and 1,9,9-trimethylcytosine<sup>4</sup> with water in Ar matrices has been described based on results obtained using a combined IR experimental and *ab initio* theoretical approach. This was a preliminary step in the investigation aimed at characterization of the H-bond interaction of the biologically more important cytosines and isocytosines with water in isolated conditions. For all the model compounds mentioned above, only a single tautomeric form is present in Ar matrices. In the following step, the combined experimental and *ab initio* results allowed us to interpret the matrix FT-IR spectra of 1-methylcytosine in water-doped Ar matrices.<sup>5</sup> We assigned the spectral features obtained for this system as originating from two different H-bonded water complexes of the amino–oxo tautomer, and one water complex of the imino–oxo (E) tautomer.

Following the 1-methylcytosine–water study, in the present work we describe the H-bond interaction of 2-hydroxypyrimidine (2HPM) and 5-bromo-2-hydroxypyrimidine (5B2HPM) and their oxo tautomers, 2-pyrimidone (2OPM) and 5-bromo-2-pyrimidone (5B2OPM), with water in Ar matrices. Contrary

to 2-hydroxypyridine and 4-hydroxypyrimidine, which also have the OH group vicinal to the ring nitrogen atom, these compounds occur predominantly as the hydroxy tautomers in Ar.<sup>6</sup> The presence of two or more tautomeric forms in comparable amounts, as for 2-hydroxypyridine<sup>7–9</sup> or for cytosine derivatives,<sup>10–13</sup> complicates the spectral assignment of the experimental absorptions, because water complexes of all these tautomers have to be considered.

Some interesting studies on 2-hydroxypyridine, its water complexes, and the water-enhanced tautomeric process in this compound in both the ground and the electronically excited states have recently appeared.<sup>14–21</sup> Also a number of theoretical and experimental studies on proton-transfer processes occurring along intra- and intermolecular H bonds in 2-hydroxypyridine and its water complexes in the ground and electronically and vibrationally excited states have been published recently.<sup>22–27</sup> In particular, Sobolewski *et al.* calculated the barrier height for the proton-transfer process in 2HPM in the ground and the electronically excited state using the CASSCF and CASPT2 *ab initio* methods.<sup>26,27</sup> This work is particularly relevant to the present study.

In the present work we demonstrate that the relative concentration of the hydroxy and oxo tautomers of 2HPM and 5B2HPM changes noticeably upon doping the isolating matrix with water. Such a solvent-assisted tautomeric transition from the hydroxy to the oxo form by a double proton-transfer process has been suggested to occur in matrices by formation of self-associates and their rearrangement involving internal hydrogen transfer.<sup>6b</sup> The shift of the tautomeric equilibrium induced by

\* Corresponding authors.

<sup>†</sup> University of Leuven.

<sup>‡</sup> University of Arizona.

<sup>§</sup> Senior Research Associate of the Belgian National Fund for Scientific Research.

**TABLE 1: Total (au) and Relative ( $\text{kJ}\cdot\text{mol}^{-1}$ ) Energies of the Hydroxy and Oxo Tautomers of 2-Hydroxypyrimidine and the 5-Halogeno Derivatives Calculated with the 6-31++G\*\* Basis Set or the BBS Basis Set<sup>a</sup>**

method	X = H		X = Br <sup>b</sup>		X = Cl		X = F	
	hydroxy	oxo	hydroxy	oxo	hydroxy	oxo	hydroxy	oxo
SCF	-337.5874643	-337.5820415	-2909.3516372	-2909.3434037	-796.4817159	-796.4731843	-436.4329028	-436.4229334
MP2 <sup>b</sup>	-338.6131794	-338.6063259	2910.6275222	-2910.6178818	-797.6324585	-797.6225754	-437.6236118	-437.6116968
ZPE <sup>c</sup>	0.0883348	0.0882529	0.06989013	0.06985296	0.07046946	0.07043562	0.07165755	0.07159896
total	-338.5248446	-338.5180735	-2910.557632	-2910.548028	-747.561989	-747.5521398	-437.5519543	-437.5400978
$\Delta E_{\text{T}}^{\text{d}}$	0.00	17.79	0.00	25.22	0.00	25.86	0.00	31.13
$\mu$ (D)	3.07	6.82	1.81	5.46	1.72	5.29	1.78	5.26
$K_{\text{T}}(298.15\text{ K})^{\text{e}}$	1308		26350		33914		284201	

<sup>a</sup> Geometries optimized at the SCF/6-31++G\*\* or BBS level of theory (X is the substituent at the C<sub>5</sub> position). <sup>b</sup> Only valence correlation is considered. <sup>c</sup> Calculated as  $0.9\sum h\nu_i$ . <sup>d</sup> Energy difference between tautomers of one compound. <sup>e</sup>  $-RT \ln K_{\text{T}} \approx \text{DET}$ . <sup>f</sup> BBS basis set used (see text).

environment is usually explained by the difference in the dipole–dipole or dipole–induced dipole interactions of the tautomers with the solvent molecules. The dominance of the oxo tautomer in the polar environment is thus explained by its larger dipole–dipole interaction with solvent molecules than for the hydroxy tautomer. This interaction shifts the tautomeric equilibrium from the hydroxy form to the oxo form. This is also the reason why 2HPM occurs as the oxo tautomer in the crystalline state and in polar solvents,<sup>28,29</sup> but as the hydroxy tautomer in the gas phase and in Ar matrices.<sup>30</sup>

The *ab initio* assisted analysis of the FT-IR spectra of 2HPM and 5B2HPM in water-doped matrices presented in this work provides an insight into the H-bond properties of hydroxy tautomers of heterocyclic compounds with the OH group vicinal to the nitrogen atom in the pyrimidine ring. In particular, the present results will allow in the future investigations to discriminate between the H-bonded complexes formed by the hydroxy and oxo tautomers of cytosine derivatives.<sup>13</sup>

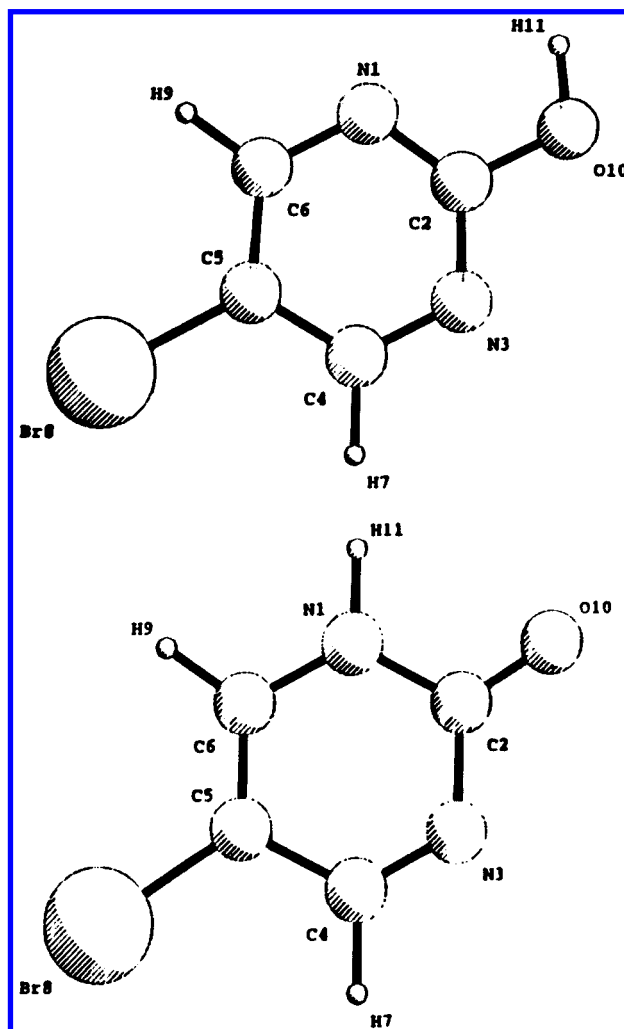
## Methodology

**Experimental Method.** A detailed description of the experimental method used here has been presented elsewhere.<sup>31,32</sup> Optimal sublimation temperatures were 55 and 75 °C for 2HPM and 5B2HPM, respectively, at the Ar deposition rate of 5 mmol/h. Similar to all our earlier studies on water complexes in Ar,<sup>1–5</sup> the water-to-base ratio varying between 1:1 and 5:1 was used. The latter ratio ensures an excess amount of the 1:1 complex species to be present in the matrix with only weak spectral manifestations of higher-stoichiometry complexes.

2HPM was obtained from 2HPM·HCl, purchased from Janssen Chimica, by using the neutralization method described by Hunt.<sup>33</sup> In a modified method of Wheeler,<sup>34</sup> used to prepare 5B2HPM, the parent base 2HPM was dissolved in the solution of 80 vol % acetic acid and 20 vol % acetic acid anhydride, and bromine was added slowly during refluxation. The precipitate was filtered and washed with acetic acid, and the compound was recrystallized from ethanol. The purity of both synthesized compounds was checked with NMR, mass spectrometry, and IR spectroscopy in KBr dispersion, and they were found to be >99% pure. Twice-distilled water was used for the water-doped samples, while Ar gas (99.9949%) from Air Liquide was used in all experiments.

**Theoretical Method.** Optimized geometries of the hydroxy and oxo tautomers of 2HPM, 5F2HPM (5-fluoro-2-hydroxypyrimidine), and 5C2HPM (5-chloro-2-hydroxypyrimidine) were determined at the SCF/6-31++G\*\* level of theory. In the case of 5B2HPM, the standard 6-31++G\*\* basis set was used for H, C, N, and O atoms, while for the Br atom the double zeta basis set from Ahlrichs<sup>35</sup> with the contraction scheme (14s11p5d)/[8s6p2d] was used. The Ahlrichs basis for Br was augmented

## SCHEME 1



with an additional polarization function taken from Huzinaga *et al.*,<sup>36</sup> and this basis set is further referred to as the “BBS” basis set. In all the calculations, the d-shells had six Cartesian compounds. The IR frequencies and intensities and the zero-point vibrational energy (ZPE) were computed at the SCF level of theory using the analytical derivative procedure incorporated in the Gaussian 92 program.<sup>37</sup> Following these calculations, the total energies of the tautomers were calculated at the MP2+0.9ZPE level using the same basis set (the Møller–Plesset second-order energy was calculated with the SCF/6-31++G\*\* optimal geometry; MP2/6-31++G\*\*//SCF/6-31++G\*\*). Calculated frequencies were scaled down by the single factor 0.90 to approximately correct for vibrational anharmonicity, as well as for the overestimation of the force constants at the SCF level.

**TABLE 2: Experimental (Ar Matrix) and Calculated (SCF/6-31++G\*\*) IR Spectral Data for 2-Hydroxypyrimidine**

experimental		calculated		PED <sup>c</sup>
$\nu$ (cm <sup>-1</sup> )	$I^a$ (km·mol <sup>-1</sup> )	$\nu^b$ (cm <sup>-1</sup> )	$I$ (km·mol <sup>-1</sup> )	
3591/3588	151 <sup>f</sup>	3742	151	$\nu(\text{OH})$ (100)
3075	1	3062	5	$\nu(\text{C}_5\text{H})$ (92)
3050	2.5	3024	22	$\nu(\text{C}_6\text{H})$ (75) + $\nu(\text{C}_4\text{H})$ (23)
3015	3.5	3019	12	$\nu(\text{C}_4\text{H})$ (73) + $\nu(\text{C}_6\text{H})$ (20)
1591	112	1627	292	$\nu(\text{C}_5\text{C}_6)$ (21) + $\nu(\text{C}_2\text{N}_3)$ (17) + $\nu(\text{C}_6\text{N}_1)$ (19) + $\nu(\text{N}_3\text{C}_4)$ (13) + $\delta(\text{C}_6\text{H})$ (12)
1573	105	1614	289	$\nu(\text{C}_4\text{C}_5)$ (24) + $\nu(\text{N}_1\text{C}_2)$ (21) + $\nu(\text{N}_3\text{C}_4)$ (12) + $\delta(\text{C}_4\text{H})$ (11)
1470/1467	111 <sup>f</sup>	1464	244	$\nu(\text{C}_2\text{O})$ (19) + $\delta(\text{C}_4\text{H})$ (15) + $\delta(\text{C}_5\text{H})$ (14) + $\nu(\text{C}_2\text{N}_3)$ (12)
1435/1433	255 <sup>f</sup>	1450	261	$\delta(\text{C}_5\text{H})$ (21) + $\delta(\text{C}_6\text{H})$ (20) + $\nu(\text{C}_2\text{O})$ (12) + $\nu(\text{N}_1\text{C}_2)$ (11)
1353	86	1342	12	$\nu(\text{C}_2\text{O})$ (26) + $\delta(\text{C}_4\text{H})$ (22) + $\delta(\text{C}_6\text{H})$ (15) + $\nu(\text{N}_3\text{C}_4)$ (13) + $\nu(\text{N}_1\text{C}_6)$ (11) + $\delta_{\text{R1}}$ (11)
1333/1325	142 <sup>f</sup>	1324	78	$\delta(\text{OH})$ (32) + $\delta(\text{C}_4\text{H})$ (30) + $\delta(\text{C}_6\text{H})$ (28)
1210/1197	144 <sup>f</sup>	1185	130	$\delta(\text{OH})$ (48) + $\delta(\text{C}_6\text{H})$ (12)
1168	60	1139	20	$\delta(\text{C}_5\text{H})$ (32) + $\nu(\text{C}_6\text{N}_1)$ (26) + $\nu(\text{N}_3\text{C}_4)$ (25) + $\nu(\text{N}_1\text{C}_2)$ (10) + $\nu(\text{C}_2\text{N}_3)$ (10)
1090	11	1062	0.3	$\nu(\text{C}_5\text{C}_6)$ (40) + $\nu(\text{C}_4\text{C}_5)$ (20) + $\delta(\text{C}_6\text{H})$ (12) + $\delta(\text{C}_4\text{H})$ (10)
1080	21	1043	29	$\nu(\text{C}_4\text{C}_5)$ (35) + $\delta(\text{C}_5\text{H})$ (21) + $\nu(\text{N}_1\text{C}_2)$ (19) + $\nu(\text{C}_5\text{C}_6)$ (15)
1023	17	1019	0	$\gamma(\text{C}_4\text{H})$ (64) + $\gamma(\text{C}_6\text{H})$ (43)
<i>d</i>		1006	0.02	$\gamma(\text{C}_6\text{H})$ (54) + $\gamma(\text{C}_4\text{H})$ (33) + $\gamma(\text{C}_5\text{H})$ (27)
995	5	987	1	$\delta_{\text{R1}}$ (54) + $\nu(\text{C}_2\text{N}_3)$ (10)
871	42	870	16	$\nu(\text{C}_2\text{O})$ (26) + $\nu(\text{C}_2\text{N}_3)$ (20) + $\delta_{\text{R1}}$ (19) + $\nu(\text{N}_1\text{C}_2)$ (17)
808	69	818	57	$\gamma(\text{C}_2\text{O})$ (55) + $\tau_{\text{R1}}$ (48)
793	11	794	38	$\gamma(\text{C}_5\text{H})$ (77)
641	17	632	7	$\delta_{\text{R2}}$ (67) + $\delta_{\text{R3}}$ (17)
572	3	584	1	$\delta_{\text{R3}}$ (61) + $\delta_{\text{R2}}$ (16) + $\nu(\text{C}_2\text{O})$ (14)
536	52	534	18	$\tau_{\text{R1}}$ (38) + $\gamma(\text{OH})$ (26) + $\gamma(\text{C}_2\text{O})$ (24) + $\tau_{\text{R2}}$ (14)
504/501	193 <sup>f</sup>	493	120	$\gamma(\text{OH})$ (73) + $\gamma(\text{C}_2\text{O})$ (11)
453	6	448	19	$\delta(\text{C}_2\text{O})$ (80)
405	30	415	1	$\tau_{\text{R3}}$ (107)
<i>e</i>		199	5	$\tau_{\text{R2}}$ (87)

<sup>a</sup> Experimental intensities normalized to the calculated value of  $\nu(\text{OH})$  (151 km·mol<sup>-1</sup>). <sup>b</sup> Uniform scaling factor 0.90. <sup>c</sup> Only contributions  $\geq 10\%$  are listed;  $\nu$  designates stretching,  $\delta$  in-plane bending,  $\gamma$  out-of-plane deformation and  $\tau$  torsion; subscript R = ring mode. <sup>d</sup> Too weak to be observed. <sup>e</sup> Situated below studied region ( $< 400$  cm<sup>-1</sup>). <sup>f</sup> Total intensity of band pair (main band of pair in italics).

The same procedure was also applied to the H-bonded complexes with water. In determining the H-bond energies, the basis set superposition error (BSSE) was corrected by recalculating the monomer energies in the basis set of the heterodimer (counterpoise correction). Detailed arguments for the use of the above approach have been described earlier.<sup>1</sup>

## Results and Discussion

**2HPM and 5B2HPM.** Table 1 summarizes the theoretical results obtained for the hydroxy  $\rightleftharpoons$  oxo tautomerism in 2HPM and 5B2HPM. For sake of comparison, calculations have also been performed for the 5F and the 5Cl derivatives. The results clearly demonstrate that the hydroxy form (Scheme 1, 5B2HPM) is by far the most stable tautomer in each case, with the energy difference to the less stable oxo form increasing with increasing electronegativity of the halogen substituent at the ring C<sub>5</sub> position. These results are consistent with *ab initio* and experimental data for cytosines and 5-X-cytosines, which exhibit the same trend: *i.e.*, the hydroxy form is stabilized by an electron-withdrawing halogen atom at the ring C<sub>5</sub> position.<sup>38</sup>

The (Ar) matrix IR spectrum of 2HPM has already been described several times in the literature, but its spectrum was analyzed by comparison with CNDO and lower level *ab initio* (SCF/3-21G) results only.<sup>6d</sup> The experimental and theoretical vibrational data for the hydroxy form obtained in this work are summarized in Table 2. The theoretical results for the oxo tautomer are summarized in Table 3. From the experimental FT-IR spectrum (Figure 1), it is evident that the hydroxy tautomeric form is highly predominant in Ar, in agreement with the earlier investigations.<sup>6</sup> This is manifested by the observation of an intense, splitted  $\nu_{\text{OH}}$  absorption at 3591 cm<sup>-1</sup>, while there are only some very weak bands in the  $\nu_{\text{N-H}}$  (3500–3400 cm<sup>-1</sup>) and the  $\nu_{\text{C=O}}$  region (1770–1700 cm<sup>-1</sup>). The latter feature is characteristic for the oxo tautomer and is normally located

around 1730 cm<sup>-1</sup> for monomeric nucleic bases and their analogs.<sup>7,10–13,32,39</sup> If the oxo tautomer is present in the sample, the  $\nu_{\text{C=O}}$  mode is usually very intense. Our assignment of the weak bands in the 3500–3400 and 1770–1700 cm<sup>-1</sup> regions in the oxo tautomer is tentative. It is also possible that these bands may be due to impurities in the sample. Provided that our assignment is correct, we can use the combination of the experimental and *ab initio* calculated intensities of the characteristic  $\nu_{\text{OH}}$  and  $\nu_{\text{C=O}}$  modes to estimate the value of the tautomerization constant  $K_{\text{T}}(\text{h/o})$ ,<sup>10–12</sup> but due to the very small experimental intensity of the  $\nu_{\text{C=O}}$  band(s), only the order of magnitude of its value can be obtained in the present case. Table 4 summarizes these experimental  $K_{\text{T}}(\text{h/o})$  estimations. Taking into account the earlier reported value of  $\pm 300$  by Lapinski *et al.*,<sup>6d</sup> which was obtained by taking into account only the main  $\nu_{\text{C=O}}$  component of the experimental Fermi-resonance multiplet, and a rather large estimated theoretical intensity ratio of the C=O, and OH vibrations of 10.0, the value of  $\pm 60$  obtained for 2HPM in this work is not in conflict with the earlier results. We may therefore conclude that 2HPM occurs in the gas phase and in matrices predominantly as the hydroxy tautomer, in agreement with the *ab initio* data listed in Table 1. As far as the assignment of the experimental spectrum of the 2HPM monomer is concerned, except for a very weak  $\gamma_{\text{CH}}$  mode and one ring torsion situated below the studied region, all fundamentals of 2HPM are rather easily assigned by comparison with the theoretical data. The mean frequency deviation  $|\nu^{\text{exp}} - \nu^{\text{th}}|$  (the  $\nu_{\text{OH}}$  mode has been omitted because of its larger anharmonicity<sup>3</sup>) for the assignment is 13.6 cm<sup>-1</sup>, which is the usual level of accuracy obtained for cytosine analogs using the SCF/6-31++G\*\* level of theory.<sup>1–5</sup> However, the deviations between experimental and predicted intensities are larger than observed for most other cytosine-modeling molecules studied so far.

TABLE 3: Calculated (SCF/6-31++G\*\*) IR Spectral Data for 2-Pyrimidone

calculated		PED <sup>a</sup>
$\nu^a$ (cm <sup>-1</sup> )	$I$ (km <sup>2</sup> mol <sup>-1</sup> )	
3484	78	$\nu(\text{NH})$ (100)
3076	12	$\nu(\text{C}_5\text{H})$ (88) + $\nu(\text{C}_6\text{H})$ (11)
3048	3	$\nu(\text{C}_6\text{H})$ (89) + $\nu(\text{C}_5\text{H})$ (11)
2996	27	$\nu(\text{C}_4\text{H})$ (99)
1762	1097	$\nu(\text{C}_2\text{O})$ (77)
1665	155	$\nu(\text{N}_3\text{C}_4)$ (36) + $\nu(\text{C}_5\text{C}_6)$ (27)
1563	296	$\nu(\text{C}_5\text{C}_6)$ (21) + $\nu(\text{N}_3\text{C}_4)$ (18) + $\delta(\text{NH})$ (16) + $\nu(\text{C}_4\text{C}_5)$ (11)
1456	35	$\nu(\text{C}_6\text{N}_1)$ (24) + $\delta(\text{NH})$ (18) + $\delta(\text{C}_6\text{H})$ (15) + $\delta(\text{C}_5\text{H})$ (13) + $\nu(\text{N}_3\text{C}_4)$ (13)
1410	46	$\delta(\text{C}_4\text{H})$ (23) $\delta(\text{NH})$ (17) + $\delta(\text{C}_6\text{H})$ (17) + $\nu(\text{C}_4\text{C}_5)$ (13) + $\delta(\text{C}_5\text{H})$ (12)
1353	48	$\delta(\text{C}_4\text{H})$ (41) + $\delta(\text{NH})$ (17) + $\nu(\text{N}_3\text{C}_4)$ (14) + $\delta(\text{C}_5\text{H})$ (12)
1178	53	$\delta(\text{C}_6\text{H})$ (39) + $\nu(\text{C}_6\text{N}_1)$ (23) + $\delta(\text{NH})$ (14) + $\nu(\text{C}_5\text{C}_6)$ (11)
1154	21	$\nu(\text{N}_1\text{C}_2)$ (29) + $\nu(\text{C}_2\text{N}_3)$ (28) + $\delta(\text{C}_4\text{H})$ (14) + $\delta(\text{C}_5\text{H})$ (11)
1088	13	$\delta(\text{C}_5\text{H})$ (33) + $\nu(\text{C}_6\text{N}_1)$ (26) + $\nu(\text{C}_5\text{C}_6)$ (23)
1011	0.03	$\gamma(\text{C}_4\text{H})$ (84) + $\gamma(\text{C}_6\text{H})$ (22)
990	0.02	$\gamma(\text{C}_6\text{H})$ (72) + $\gamma(\text{C}_5\text{H})$ (25) + $\gamma(\text{C}_4\text{H})$ (17)
985	25	$\delta_{\text{R1}}$ (72) + $\nu(\text{C}_4\text{C}_5)$ (11)
974	10	$\nu(\text{C}_4\text{C}_5)$ (55) + $\delta_{\text{R1}}$ (18)
817	11	$\nu(\text{C}_2\text{N}_3)$ (45) + $\nu(\text{N}_1\text{C}_2)$ (30)
799	87	$\gamma(\text{C}_2\text{O})$ (80) + $\tau_{\text{R1}}$ (19)
755	46	$\gamma(\text{C}_5\text{H})$ (76) + $\gamma(\text{C}_6\text{H})$ (12)
656	58	$\gamma(\text{NH})$ (85) + $\tau_{\text{R1}}$ (19)
614	1	$\delta_{\text{R2}}$ (60) + $\delta_{\text{R3}}$ (13)
557	7	$\delta_{\text{R3}}$ (66) + $\delta_{\text{R2}}$ (19)
483	2	$\delta(\text{C}_2\text{O})$ (68)
473	40	$\tau_{\text{R1}}$ (45) + $\tau_{\text{R2}}$ (24) + $\gamma(\text{NH})$ (18) + $\gamma(\text{C}_2\text{O})$ (16)
382	1	$\tau_{\text{R3}}$ (106)
134	1	$\tau_{\text{R2}}$ (86) + $\tau_{\text{R1}}$ (19)

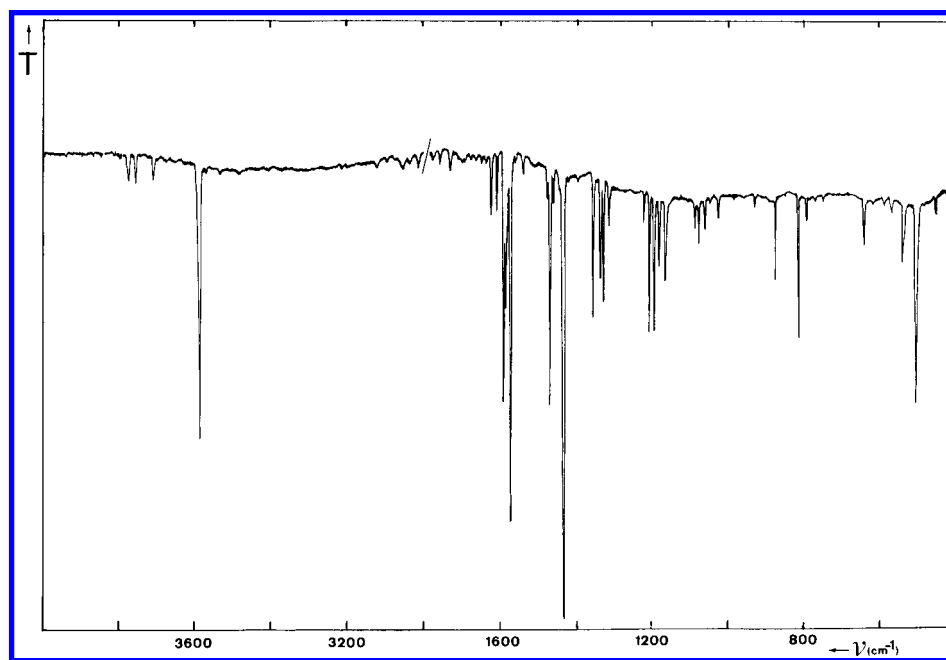
<sup>a</sup> See Table 2, footnotes *b* and *c*.

Figure 1. FT-IR spectrum of 2-hydroxypyrimidine isolated in Ar at 12 K.

Figure 2 illustrates the FT-TR spectrum of 5BHPM in Ar. Again it is obvious that the hydroxy tautomer is highly predominant for this compound, since no  $\nu_{\text{NH}}$  band is observed (region 3500–3400 cm<sup>-1</sup>) and only a very weak band is found in the  $\nu_{\text{C=O}}$  region around 1732 cm<sup>-1</sup>. Multiplying the intensity ratio of the strong  $\nu_{\text{OH}}$  band (3590 cm<sup>-1</sup>) and the weak  $\nu_{\text{C=O}}$  band by the inverse ratio of the theoretically predicted intensities, an estimated  $K_{\text{T}}(\text{h/o})$  value of 184 is obtained (Table 4). As can be seen by comparing the data in Table 4 with the data in Table 1, there is a dramatical difference between the experimentally estimated  $K_{\text{T}}(\text{h/o})$  values and their predicted values obtained from the approximate relation:  $-RT \ln K_{\text{T}} =$

$\Delta E_{\text{T}}$ , where the energy difference between the oxo and hydroxy tautomers,  $\Delta E_{\text{T}}$ , is taken from the theoretical calculations. Interestingly, for 1-CH<sub>3</sub>-cytosine<sup>5</sup> and 1-CH<sub>3</sub>-adenine,<sup>40</sup> much smaller differences between predicted and experimental  $K_{\text{T}}$  values were observed. We will comment on the unusually large difference between the experimental and theoretical  $K_{\text{T}}$  value of 2HPM and 5BHPM in the Discussion Session.

Table 5 lists the experimental frequencies and intensities of the predominant hydroxy tautomer 5B2HPM in comparison with the *ab initio* predicted spectral parameters. Again, the assignment can be performed for almost all the fundamentals, and the mean frequency deviation is 14.3 cm<sup>-1</sup> ( $\nu_{\text{OH}}$  mode omitted).



**TABLE 4: Experimental Estimation of the Lower Limit  $K_T(h/o)$  Value for 2-Hydroxypyrimidine (2HPM)  $\rightleftharpoons$  2-Pyrimidone (2OPM) and 5-Bromo-2-hydroxypyrimidine (5B2HPM)  $\rightleftharpoons$  5-Bromo-2-pyrimidone (5B2OPM)**

band pair		$A(\nu_{\text{h}})/A(\nu_{\text{o}})$	$a(\nu_{\text{o}})/a(\nu_{\text{h}})^a$	$K_{\text{T}}(\text{h/o})$
$\nu_{\text{h}} (\text{cm}^{-1})$	$\nu_{\text{o}} (\text{cm}^{-1})$			
2HPM $\rightleftharpoons$ 2OPM				
$\nu_{\text{OH}}$ (3591)	$\nu_{\text{CO}}$ (1730)	18.8	7.3	138
$\nu_{\text{OH}}$ (3591)	$\nu_{\text{CO}}$ (1730/1719/1713)	8.2	7.3	60
literature <sup>6d</sup>		29.5 <sup>b</sup>	10.0 <sup>c</sup>	295
5B2HPM $\rightleftharpoons$ 5B2OPM				
$\nu_{\text{OH}}$ (3590)	$\nu_{\text{CO}}$ (1732)	26.3	7.0	184

<sup>a</sup> Theoretical intensities taken from Tables 2 (2HPM) and 3 (2OPM) or from Table 5 (5B2HPM), with  $a_{\text{C=O}}$  (5B2OPM) = 1209  $\text{km}\cdot\text{mol}^{-1}$ .

<sup>b</sup> Only the main  $\nu(\text{CO})$  component has been taken into account.<sup>6d</sup>

<sup>c</sup> Crudely estimated theoretical intensity ratio.<sup>6d</sup>

Similar to the observation made for 2HPM, some rather large deviations between experimental and predicted intensities are noted.

**2HPM/H<sub>2</sub>O/Ar and 2B2HPM/H<sub>2</sub>O/Ar.** In view of the close similarity between 2HPM and 5B2HPM, the spectral results for the two molecules will be presented together, while *ab initio* results are only discussed for the nonsubstituted compound.

The hydroxy tautomer has three basic sites: the two heterocyclic nitrogen atoms and the oxygen atom of the OH group. On the other hand, the only proton-donor site available is the hydrogen atom of the OH group. If the tautomeric equilibrium is shifted from the hydroxy form toward the oxo form in the presence of water, two additional H-bond interaction sites of the oxo tautomer, *i.e.*, the basic C<sub>2</sub>=O group and the acidic N<sub>1</sub>-H group, should also be taken into account. The proton affinity (PA) of 2-pyrimidone was estimated to be 870  $\text{kJ}\cdot\text{mol}^{-1}$ .<sup>41</sup> Although ref 41 does not mention if this value refers to the nitrogen atom or to the C<sub>2</sub>=O site, it was demonstrated that both sites have very similar calculated PA values in 2-pyridone.<sup>42</sup>

The *ab initio* geometry optimizations performed for complexes of 2HPM and 2OPM with a water molecule indicate that the closed structure with two H bonds between the base and

water (Scheme 2) is the most stable 1:1 complex for both systems (Table 6). The H bond energies calculated at the MP2/6-31++G\*\*//SCF/6-31++G\*\* level of theory, corrected for the BSSE, are 49 and 60  $\text{kJ}\cdot\text{mol}^{-1}$  for 2HPM and 2OPM, respectively. These values manifest a strong H-bonding association in both complexes. As a matter of fact, the H-bond interaction energies for the N $\cdots$ H-O $\cdots$ HO complex of 2HPM can be compared with the values obtained earlier at the same level of theory for the singly H-bonded N $\cdots$ HO-H pyrimidine water complex and the O-H $\cdots$ OH<sub>2</sub> 4-hydroxypyridine-water complex, the interaction energies being 18 and 25  $\text{kJ}\cdot\text{mol}^{-1}$ , respectively. The difference in the interaction energies of the singly- and doubly H-bonded complexes indicates that H-bond cooperativity definitely exists between the two H-bonds in the closed 1:1 complex. This point is discussed further. Another important result emerging from the *ab initio* calculations is that the energy difference between the 2HPM and 2OPM tautomers drops by half from 18  $\text{kJ}\cdot\text{mol}^{-1}$  in the free base (Table 1) to 9  $\text{kJ}\cdot\text{mol}^{-1}$  in the complex with water.

The experimental FT-IR spectra of 2HPM and 5B2HPM isolated in water-doped Ar matrices (Figures 3 and 4) exhibit a series of important spectral effects induced by complexation with water. For both compounds, an intensity decrease of the bands assigned to the fundamental OH mode is observed (especially after annealing). These modes include  $\nu_{\text{OH}}$  at 3591  $\text{cm}^{-1}$ ,  $\delta_{\text{OH}}$  at 1333 and 1210  $\text{cm}^{-1}$ , and  $\gamma_{\text{OH}}$  at 504  $\text{cm}^{-1}$  (2HPM/H<sub>2</sub>O/Ar). On the other hand, the  $\nu_{\text{C=O}}$  absorption bands, at 1713/1703/1679  $\text{cm}^{-1}$  for 2HPM and at 1716/1665  $\text{cm}^{-1}$  for 5B2HPM, which were very weak in the monomer spectrum, show a clear intensity increase. This observation indicates that the tautomeric equilibrium position is noticeably shifted due to H<sub>2</sub>O doping of the matrix. A similar effect, although less pronounced, was observed for 2-hydroxypyridine and for 4-hydroxypyrimidine.<sup>21</sup> Apart from this important observation, the appearance of the following bands due to the formation of the water complex in the high-frequency region in the 2HPM case should be mentioned: *i.e.*, new  $\nu^f_{(\text{H}_2\text{O})}$  bands at 3702–3700 and 3693  $\text{cm}^{-1}$ , and new bands at 3463/3455, 3410, 3380, 3330, and 3260  $\text{cm}^{-1}$ . For 5B2HPM, similar new  $\nu^f_{\text{H}_2\text{O}}$  bands at 3701 and 3694  $\text{cm}^{-1}$ , and new absorptions at 3463/3452,

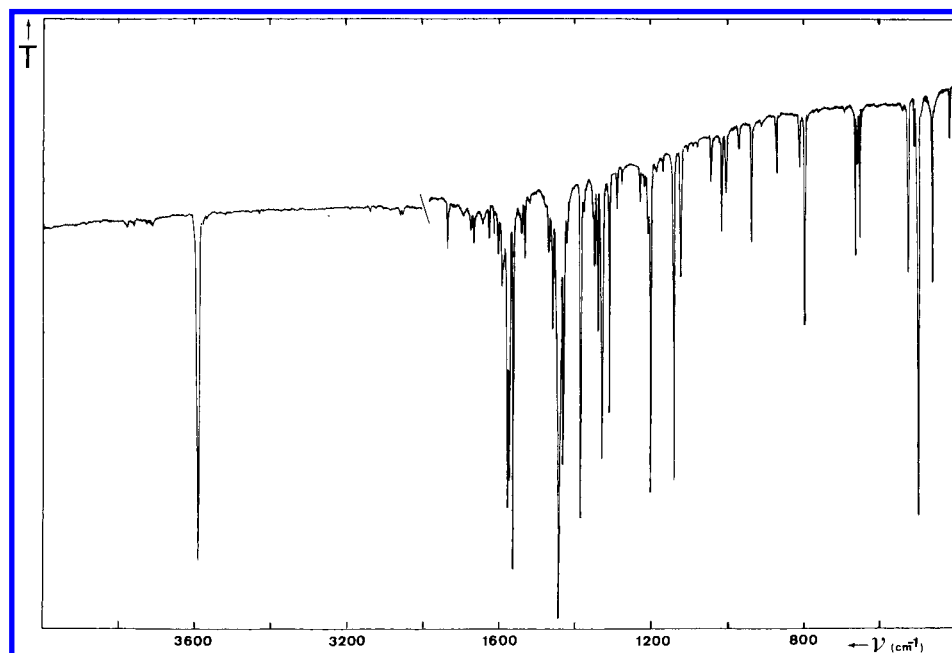


**Figure 2.** FT-IR spectrum of 5-bromo-2-hydroxypyrimidine isolated in Ar at 12 K.

**TABLE 5: Experimental (Ar Matrix) and Calculated (SCF/BBS) IR Spectral Data for 5-Bromo-2-hydroxypyrimidine**

experimental		calculated		PED <sup>c</sup>
$\nu$ (cm <sup>-1</sup> )	$I$ (km·mol <sup>-1</sup> )	$\nu^b$ (cm <sup>-1</sup> )	$I$ (km·mol <sup>-1</sup> )	
3590	172	3741	172	$\nu(\text{OH})$ (100)
3057	5	3041	4	$\nu(\text{C}_6\text{H})$ (99)
3050		3038	5	$\nu(\text{C}_4\text{H})$ (99)
1578/1574	116 <sup>f</sup>	1625	261	$\nu(\text{C}_6\text{N}_1)$ (23) + $\nu(\text{N}_3\text{C}_4)$ (19) + $\nu(\text{C}_5\text{C}_6)$ (16) + $\nu(\text{C}_2\text{N}_3)$ (13)
1563	93	1604	212	$\nu(\text{N}_1\text{C}_2)$ (23) + $\nu(\text{C}_4\text{C}_5)$ (21) + $\nu(\text{C}_2\text{N}_3)$ (14)
1445/1433	358 <sup>f</sup>	1463	628	$\nu(\text{C}_2\text{O})$ (30) + $\nu(\text{N}_1\text{C}_2)$ (17) + $\nu(\text{C}_2\text{N}_3)$ (13)
1386	63	1385	49	$\nu(\text{N}_3\text{C}_4)$ (23) + $\nu(\text{C}_6\text{N}_1)$ (18) + $\delta(\text{C}_6\text{H})$ (11) + $\nu(\text{C}_4\text{C}_5)$ (13)
1331	69	1347	22	$\nu(\text{C}_2\text{O})$ (28) + $\delta(\text{C}_4\text{H})$ (21) + $\nu(\text{C}_6\text{N}_1)$ (13) + $\nu(\text{N}_3\text{C}_4)$ (13) + $\delta(\text{C}_6\text{H})$ (13)
1311	28	1319	78	$\delta(\text{C}_6\text{H})$ (32) + $\delta(\text{C}_4\text{H})$ (34) + $\delta(\text{OH})$ (28)
1209/1203	86 <sup>f</sup>	1181	141	$\delta(\text{OH})$ (48) + $\nu(\text{C}_6\text{N}_1)$ (19) + $\nu(\text{N}_3\text{C}_4)$ (14)
1122	17	1114	16	$\nu(\text{C}_5\text{C}_6)$ (32) + $\nu(\text{C}_4\text{C}_5)$ (25) + $\nu(\text{C}_5\text{Br})$ (12) + $\delta(\text{C}_4\text{H})$ (12)
1139 <sup>d</sup>	50	1063	42	$\nu(\text{N}_1\text{C}_2)$ (28) + $\nu(\text{C}_2\text{N}_3)$ (23) + $\nu(\text{C}_4\text{C}_5)$ (22) + $\nu(\text{C}_5\text{C}_6)$ (13)
1014	10	1011	20	$\delta_{\text{R1}}$ (56) + $\nu(\text{C}_2\text{N}_3)$ (13)
1004	6	1005	0	$\gamma(\text{C}_4\text{H})$ (59) + $\gamma(\text{C}_6\text{H})$ (48)
969	3	973	6	$\gamma(\text{C}_6\text{H})$ (57) + $\gamma(\text{C}_4\text{H})$ (45)
870	6	871	1	$\nu(\text{C}_2\text{O})$ (23) + $\nu(\text{C}_2\text{N}_3)$ (20) + $\delta_{\text{R1}}$ (17) + $\nu(\text{N}_1\text{C}_2)$ (17)
797	24	813	54	$\gamma(\text{C}_2\text{O})$ (56) + $\tau_{\text{R1}}$ (49)
660	14	648	11	$\delta_{\text{R2}}$ (46) + $\nu(\text{C}_5\text{Br})$ (15) + $\nu(\text{C}_2\text{O})$ (12)
646	13	642	13	$\delta_{\text{R3}}$ (46) + $\delta_{\text{R2}}$ (24)
524	18	525	23	$\gamma(\text{OH})$ (34) + $\tau_{\text{R1}}$ (33) + $\gamma(\text{C}_2\text{O})$ (20)
495	77	489	118	$\gamma(\text{OH})$ (66) + $\gamma(\text{C}_2\text{O})$ (13) + $\tau_{\text{R1}}$ (12)
460	17	459	20	$\delta(\text{C}_2\text{O})$ (71)
413	8	415	1	$\tau_{\text{R2}}$ (79) + $\tau_{\text{R3}}$ (28)
<i>e</i>		297	1	$\gamma(\text{C}_5\text{Br})$ (69) + $\tau_{\text{R1}}$ (14)
<i>e</i>		294	0	$\nu(\text{C}_5\text{Br})$ (60) + $\delta_{\text{R3}}$ (20)
<i>e</i>		210	2	$\delta(\text{C}_5\text{Br})$ (86)
<i>e</i>		104	0	$\tau_{\text{R3}}$ (58) + $\tau_{\text{R2}}$ (19) + $\gamma(\text{C}_5\text{Br})$ (22)

<sup>a</sup> Experimental intensities normalized to the calculated value of  $\nu(\text{OH})$  (172 km·mol<sup>-1</sup>). <sup>b,c</sup> See Table 2. <sup>d</sup> Tentative assignment. <sup>e,f</sup> See Table 2.

**TABLE 6: *Ab Initio* 6-31++G\*\* Calculated Energy Components (au), Total Energy and Basis Set Superposition Error Corrected Interaction Energies (kJ·mol<sup>-1</sup>) for Closed 1:1 H-Bonded Complexes of 2-Hydroxypyrimidine and 2-Pyrimidone with H<sub>2</sub>O<sup>a</sup>**

method	2-hydroxypyrimidine...water	2-pyrimidone...water
SCF	-413.6326378	-413.6304866
MP2 <sup>a</sup>	-414.8611222	-414.8576779
ZPE <sup>b</sup>	0.1034240	0.1034172
total	-414.7576982	-414.7542607
$\Delta E^c$	0.00	9.03
dipole moment (D)	4.54	5.17
SCF + ZPE	-413.5292138	-413.5270694
MP2 + ZPE	-414.7576982	-414.7542607
SCF (base with ghose water orbitals)	-337.5899888	-337.5834830
MP2 (base with ghost water orbitals)	-338.6132562	-338.6058765
SCF (water with ghost base orbitals)	-76.0322399	-76.0320153
MP2 (water with ghost base orbitals)	-76.2349850	-76.2344931
H-bond energy (SCF + ZPE)	-51.40	-59.79
H-bond energy (MP2 + ZPE)	-55.43	-64.18
H-bond energy (SCF/BSSE + ZPE)	-42.32	-54.15
H-bond energy (MP2/BSSE + ZPE)	-48.81	-60.24

<sup>a</sup> Calculations performed with molecular structures optimized at the SCF/6-31++G\*\* level. <sup>b</sup> Only valence correlation is considered. <sup>c</sup> Calculated as  $0.9\sum h\nu_i$ . <sup>d</sup> Energy difference between isomeric complexes.

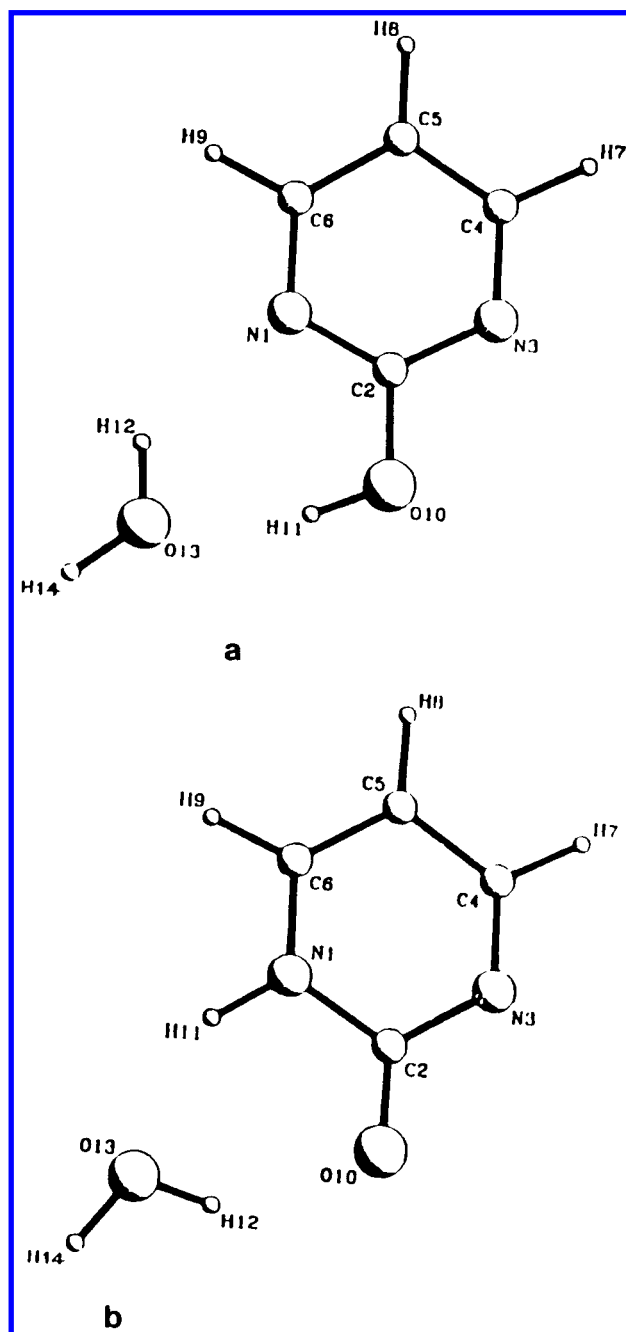
3391, 3380, 3320 and 3255 cm<sup>-1</sup>, are found. We will describe the assignment of these bands separately.

**Hydroxy Tautomer.** Since the hydroxy form is the most abundant tautomer in the matrix experiment, it can be expected that most of the new absorptions originate from formation of H-bonded water complexes of this tautomer. Figures 3 and 4 illustrate the spectra of 2HPM/H<sub>2</sub>O and 5B2HPM/H<sub>2</sub>O under different conditions. In the high-frequency region, the band observed at 3463 cm<sup>-1</sup> appears already at low H<sub>2</sub>O concentration. For 5B2HPM, the corresponding band is found at 3463 cm<sup>-1</sup>. This band of the complex can be reasonably assigned to the  $\nu_{\text{OH}}$  mode of water in an open H-bonded N...HO-H system because this intense mode, characteristic of water bonded as a proton donor to a heterocyclic nitrogen atom, has been observed before for the open N...HO-H complexes with

pyridine, pyrimidine, and 1-CH<sub>3</sub>-2-oxypyrimidine at 3400, 3468, and 3458/3449 cm<sup>-1</sup>, respectively.<sup>1,4</sup> The frequency of this mode in 2HPM is similar to its frequency in pyrimidine, but is considerably larger than that in pyridine, which is consistent with the smaller PA value of the pyrimidine nitrogen atom (PA = 888 kJ/mol) compared to the pyridine nitrogen atom (PA = 924 kJ/mol).<sup>41</sup> The  $\nu_{\text{OH}}$  absorption corresponding to the free OH bond of H-bonded water in the open H-bonded 2HPM-water complex is assigned to the band observed at 3702 cm<sup>-1</sup> in samples with low water content. This is close to the frequency of the corresponding mode in pyrimidine·H<sub>2</sub>O (3703 cm<sup>-1</sup>).<sup>1</sup>

In our former study on water complexes of 3- and 4-hydroxypyrimidine, we have observed bands characteristic of H bonding between the base OH group acting as a proton donor

SCHEME 2



toward the oxygen atom of water ( $\text{O}-\text{H}\cdots\text{OH}_2$ ) complex. Spectral manifestations of the complex were a shift of the base  $\nu_{\text{OH}}$  mode and, more interestingly, new and rather intense absorptions in the  $\nu_{\text{OH}}^{\text{f}}$  water region at 3724 and 3721  $\text{cm}^{-1}$ ,<sup>3</sup> slightly below the absorption of the proton-acceptor unit in the water dimer.<sup>43</sup> Observation of new absorptions in this spectral region in the case of 2HPM and 5B2HPM water complexes could, therefore, be also taken as a manifestation of the presence of open  $\text{O}-\text{H}\cdots\text{OH}_2$  H-bonded complexes. However, no such absorptions were found. From the thermodynamical point of view, as well as from the *ab initio* results, one expects that formation of the energetically favored, closed water complexes is more probable than of open complexes of either the  $\text{O}-\text{H}\cdots\text{OH}_2$  or the  $\text{N}\cdots\text{H}-\text{OH}$  type. However, formation of the latter type structure is only possible when the base OH bond is rotated away from the water molecule and points toward the other N atom of the pyrimidine ring. This is probably the reason why

the open  $\text{N}\cdots\text{HO}-\text{H}$  complex is observed in the experiment and the open  $\text{O}-\text{H}\cdots\text{OH}_2$  complex is not.

The perturbed water  $\nu_{\text{OH}}^{\text{b}}$  and base  $\nu_{\text{OH}}\cdots$  modes of the *ab initio* predicted, closed complex  $\text{N}_1\cdots\text{HO}\cdots\text{H}-\text{O}_{10}$  are both expected to appear in the 3400–3300  $\text{cm}^{-1}$  spectral region, because this type of complex has stronger H bonds than the corresponding open  $\text{N}\cdots\text{H}-\text{OH}$  and  $\text{H}-\text{O}\cdots\text{H}-\text{O}$  complexes. This spectral region contains water polymer bands at 3373 and 3330  $\text{cm}^{-1}$  for samples with larger water concentrations,<sup>44</sup> and their overlap with the closed-complex  $\nu_{\text{OH}}^{\text{b}}$  and  $\nu_{\text{OH}}\cdots$  bands makes assignment difficult. However, it is well-known that the intensity of the polymer band at 3330  $\text{cm}^{-1}$  is markedly smaller than that of the band at 3373  $\text{cm}^{-1}$  in  $\text{H}_2\text{O}/\text{Ar}$  matrices.<sup>44</sup> Figure 3 demonstrates that the reverse is true for 2HPM $\cdot\text{H}_2\text{O}$  and 5B2HPM $\cdot\text{H}_2\text{O}$ , and the larger intensity of the absorption at 3330  $\text{cm}^{-1}$  suggests that the  $\nu_{\text{OH}}\cdots$  absorption in the closed  $\text{N}\cdots\text{H}-\text{O}\cdots\text{H}-\text{O}$  structure overlaps with the polymer water band located there. Furthermore, the other water polymer band at 3373  $\text{cm}^{-1}$  exhibits a higher frequency shoulder at 3380  $\text{cm}^{-1}$ , for both 2HPM and 5B2HPM. Although this shoulder is also present in  $\text{H}_2\text{O}/\text{Ar}$  when a very high concentration of  $\text{H}_2\text{O}$  is used,<sup>44</sup> this band is not expected to have such a large intensity at the level of water doping used in the experiments. We therefore assign the shoulder at 3380  $\text{cm}^{-1}$  to the  $\nu_{\text{OH}}^{\text{b}}$  mode, and the band overlapping with the polymer water band at 3330  $\text{cm}^{-1}$  to the base  $\nu_{\text{OH}}\cdots$  mode in the closed  $\text{N}_1\cdots\text{H}-\text{O}\cdots\text{H}-\text{O}_{10}$  structure. We have formerly assigned the  $\nu_{\text{OH}}^{\text{b}}$  mode for  $\text{N}\cdots\text{H}-\text{O}\cdots\text{H}-\text{N}$  closed complexes of 4-aminopyrimidine<sup>2</sup> and amino-oxo 1-methylcytosine<sup>5</sup> with water to spectral features at 3386 and 3350  $\text{cm}^{-1}$ , respectively. The corresponding  $\nu_{\text{OH}}^{\text{f}}$  frequency for the closed complex should also be noticeably smaller than the corresponding mode for the open  $\text{N}\cdots\text{H}-\text{OH}$  complex, and this mode is therefore assigned to the bands found at 3693 (2HPM) and 3694 (5B2HPM)  $\text{cm}^{-1}$ . Apart from intensity decreases of the monomer bands of the base OH group, further evidence for H bonding of this group is obtained from observation of shifted bendings and out-of-plane modes, *e.g.*, for 2HPM at 1251 ( $\delta_{\text{OH}} + 41$ ), 1375 ( $\delta_{\text{OH}} + 42$ ), and 650 ( $\gamma_{\text{OH}} + 146$ )  $\text{cm}^{-1}$ . These shifts are not larger than those observed for similar modes in the 3- and 4-hydroxypyridine open  $\text{O}-\text{H}\cdots\text{O}-\text{H}$  complex, and one could argue that this is not in accordance with the expected larger shifts due to the cooperative, closed H-bond interaction. One should keep in mind, however, that the two H bonds in the closed complex are far from the perfect “H bond” geometry. As a matter of fact, the  $\text{N}\cdots\text{H}-\text{O}$  angle of the H bond in the closed complex of about 49° is much larger than the similar angle in the open  $\text{N}\cdots\text{H}-\text{OH}$  complex of pyrimidine which was predicted to be equal to 26° (in contrast to 1.7° only in pyridine $\cdot\text{H}_2\text{O}$ ).<sup>1</sup>

The other H-bond angle  $\text{O}\cdots\text{H}-\text{O}$  is 164° in the closed water–2HPM complex which is noticeably smaller than the similar angle in the open  $\text{O}\cdots\text{H}-\text{O}$  complex of 4-OH–pyridine equal to 178°. The distortion from the perfect alignment reduces the H-bond cooperativity. Table 7 summarizes the experimental and calculated frequencies for the closed complex of 2HPM. Taking into account the increased anharmonicity of the bonded OH  $\nu_{\text{OH}}^{\text{b}}$  and  $\nu_{\text{OH}}\cdots$  stretches, a good agreement between the experimental band shifts and the *ab initio* predicted shifts is observed.

**Oxo Tautomer.** The rather strong intensity increase of the  $\nu_{\text{C}=\text{O}}$  absorption shown in Figure 4 undoubtedly indicates that the abundance of the oxo tautomeric form increases when the matrix doped with water and 2HPM or 5B2HPM is annealed. This is in accordance with the *ab initio* predicted decrease of

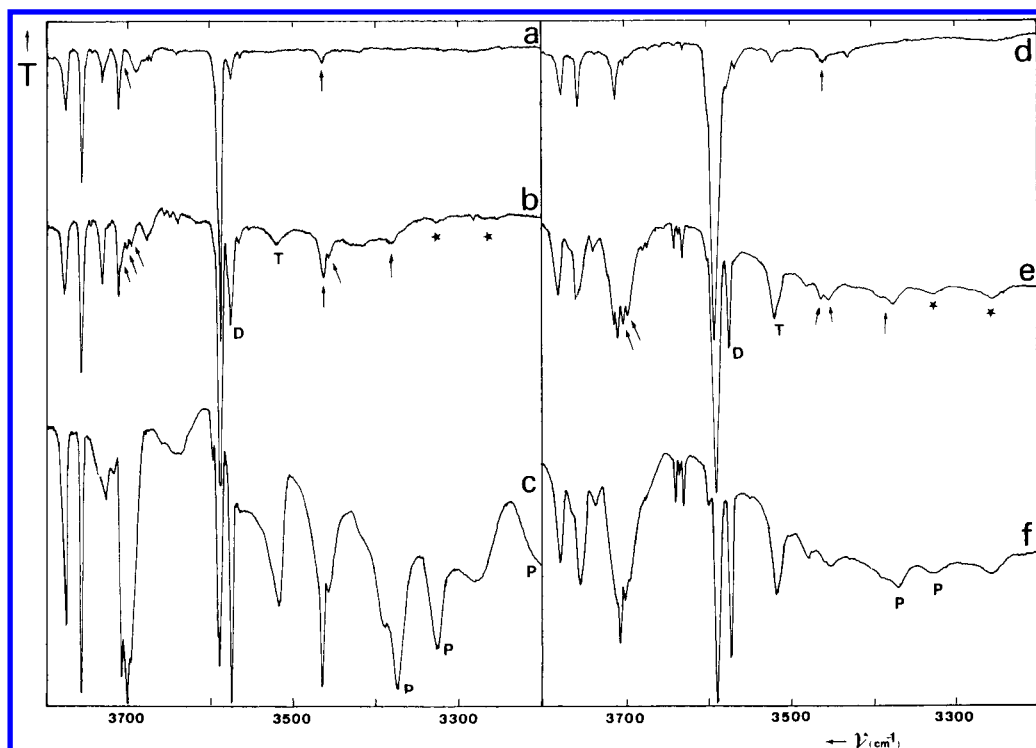


**Figure 3.** High-frequency region of the FT-IR spectrum of 2-hydroxypyrimidine/H<sub>2</sub>O/Ar (left) and 5-bromo-2-hydroxypyrimidine/H<sub>2</sub>O/Ar (right): (a) H<sub>2</sub>O/Ar = 1/500; (b) annealed a; (c) H<sub>2</sub>O/Ar = 1/100, annealed; (d) H<sub>2</sub>O/Ar = 1/1000; (e) H<sub>2</sub>O/Ar = 1/300; (f) H<sub>2</sub>O/Ar = 1/200 annealed; † = complex H<sub>2</sub>O modes; \* = shifted base modes; D,T,P = water dimer, trimer, polymer bands.

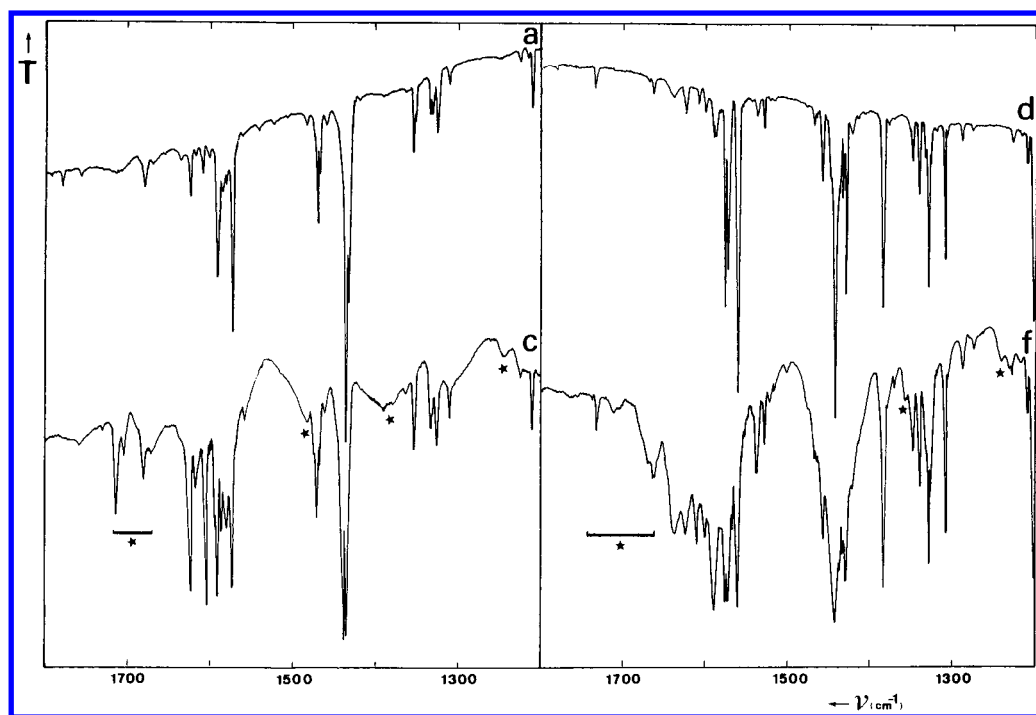


**Figure 4.** Carbonyl stretching region of the FT-IR spectrum of 2-hydroxypyrimidine/H<sub>2</sub>O/Ar (left) and 5-bromo-2-hydroxypyrimidine/H<sub>2</sub>O/Ar (right): (a, c, d, f) see Figure 3; \* = shifted base modes, \* = appearance of  $\nu_{C=O}$  mode(s); D,T,P = water dimer, trimer, polymer bands.

the energy difference between the 2HPM and 2OPM tautomers from 18 to 9 kJ/mol<sup>-1</sup> when they are complexed with water. The bands observed for the H-bonded complexes of the oxo tautomer are predominantly those of the doubly H-bonded complex of this tautomer (see Scheme 2h). Prominent complex bands of 2OPM to be assigned are those observed at 3260, 1713/1703/1679, 1440, 826, and 760 cm<sup>-1</sup>. These bands can respectively be attributed to the  $\nu_{NH\cdots}$ ,  $\nu_{C=O\cdots}$  (with Fermi components),  $\delta_{NH\cdots}$ ,  $\gamma_{C=O\cdots}$ , and  $\gamma_{NH\cdots}$  modes of the complex.

We mentioned earlier the observation of the intense doublet band at 3463/3455 cm<sup>-1</sup> for both 2HPM·H<sub>2</sub>O and 5B2HPM·H<sub>2</sub>O. The higher-frequency component of this doublet was assigned to  $\nu_{OH}^b$  in the open N $\cdots$ H—OH complex of the hydroxy tautomer. The other component of the doublet is most probably due to the  $\nu_{OH}^b$  mode in the closed C=O $\cdots$ H—O $\cdots$ H—N complex. This latter mode is expected to exhibit a rather broad absorption, as was the case for 2-pyridone·H<sub>2</sub>O,<sup>13</sup> and one may wonder why, in the present case, the width of this mode is so



**TABLE 7: Experimental (Ar Matrix) and Calculated (SCF/6-31++G\*\*) IR Spectral Data for the Closed N<sub>1</sub>⋯H—O⋯H—O<sub>10</sub> H-Bonded Complex of 2-Hydroxypyrimidine with Water**

experimental		calculated			optimal scaling <sup>c</sup>	PED <sup>d</sup>
$\nu$ (cm <sup>-1</sup> )	$\Delta\nu$ (cm <sup>-1</sup> ) <sup>a</sup>	$\nu$ (cm <sup>-1</sup> ) <sup>b</sup>	$I$ (km•mol <sup>-1</sup> )	$\Delta\nu$ (cm <sup>-1</sup> ) <sup>a</sup>		
Water Modes						
3693	-41	4239	187	-28	0.870	$\nu^f(\text{OH})$ (88) + $\nu^b(\text{OH})$ (13)
3380	-299	4082	222	-64	0.828	$\nu^b(\text{OH})$ (84) + $\nu^f(\text{OH})$ (12)
1620	+29	1743	154	+13	0.929	$\delta(\text{HOH})$ (96)
565?		578	89			$\delta(\cdots\text{OHH}\cdots)$ (54)
Base Modes						
3330	-261	3588	478	-179	0.833 (0.840) <sup>e</sup>	$\nu(\text{OH})$ (96)
1476	+6	1471	297	+8		$\nu(\text{C}_2\text{O})$ (26) + $\delta(\text{C}_4\text{H})$ (11) + $\nu(\text{C}_2\text{N}_3)$ (11)
1375	+42	1356	125	+31		$\delta(\text{OH})$ (47) + $\delta(\text{C}_5\text{H})$ (31)
1251	+41	1226	83	+41		$\delta(\text{OH})$ (26) + $\delta(\text{C}_6\text{H})$ (20)
810	+2	821	67	+3		$\gamma(\text{C}_2\text{O})$ (57) + $\tau_{\text{R}}$ (48)
650	+146	708	186	+215		$\gamma(\text{OH})$ (94)

<sup>a</sup> Shift with respect to experimental or calculated monomer frequencies (Table 2); calculated monomer water frequencies are 4267, 4146, and 1730 cm<sup>-1</sup>; for  $\nu^b_{\text{OH}}$ , the experimental shift is corrected for (reduced) coupling in bonded water.<sup>48</sup> <sup>b</sup> Water modes unscaled, base modes uniformly scaled with 0.90. <sup>c</sup> Optimal scaling factor obtained from  $\nu^{\text{exp}}/\nu^{\text{th}}$ . <sup>d</sup> Only contributions >10 are listed; description of intermolecular modes as in 4-NH<sub>2</sub>-pyrimidine·H<sub>2</sub>O.<sup>2</sup> <sup>e</sup> Value for the free base  $\nu_{\text{OH}}$  mode.

**TABLE 8: Experimental (Ar Matrix) and Calculated (SCF/6-31++G\*\*) IR Spectral Data for the Closed C<sub>2</sub>=O⋯H—O⋯H—N<sub>1</sub> H-Bonded Complex of 2-Pyrimidone with Water**

experimental		calculated		$\Delta\nu$ (cm <sup>-1</sup> ) <sup>a</sup>	optimal scaling <sup>c</sup>	PED <sup>d</sup>
$\nu$ (cm <sup>-1</sup> )	$\Delta\nu$ (cm <sup>-1</sup> ) <sup>a</sup>	$\nu$ (cm <sup>-1</sup> ) <sup>b</sup>	$I$ (km•mol <sup>-1</sup> )			
Water Modes						
3700	−34	4238	157	−29	0.873	$\nu^f(\text{OH})$ (88) + $\nu^b(\text{OH})$ (13)
3455	−217	4025	224	−121	0.858	$\nu^b(\text{OH})$ (84) + $\nu^f(\text{OH})$ (12)
1618	+27	1739	425	+9	0.930	$\delta(\text{HOH})$ (96)
560?		600	196			$\delta(\cdots\text{OHH}\cdots)$ (65)
Base Modes						
3260	<i>e</i>	3392	334	−92	0.865	$\nu(\text{N}_1\text{H})$ (99)
1679	−34?	1736	1080	−26		$\nu(\text{C}_2\text{O})$ (65) + $\delta(\text{N}_1\text{H})$ (12)
1440	<i>e</i>	1469	90	+13		$\delta(\text{N}_1\text{H})$ (24) + $\nu(\text{C}_6\text{N}_i)$ (16) + $\nu(\text{N}_3\text{C}_4)$ (14)
826	<i>e</i>	811	141	+12		$\gamma(\text{C}_2\text{O})$ (84) + $\gamma(\text{N}_1\text{H})$ (27)
760	<i>e</i>	766	17	+110		$\gamma(\text{N}_1\text{H})$ (65) + $\tau_{\text{R}}$ (22) + $\gamma(\text{C}_5\text{H})$ (14)

<sup>a-d</sup> See Table 7. <sup>e</sup> Experimental shift not available because of very low abundance of the free tautomer 2OPM.

small. Furthermore, for pyrimidine and 1-methyl-2-pyrimidone, the  $\nu^b_{\text{OH}}$  bands of the open N⋯H—OH complexes also exhibited a doublet structure, which was explained by two different orientations of the free OH bond of complexed water with respect to the pyrimidine ring. The latter is rather unlikely in the pyrimidine derivative with the hydroxy group adjacent to the nitrogen atom, since the orientation of this group toward the vicinal nitrogen atom should strongly favor formation of the closed N⋯H—O⋯H—O complex. We therefore interpret the doublet character of the bands at 3463/3455 cm<sup>-1</sup> for 2HPM and 5B2HPM as a combination of a relatively sharp  $\nu^b_{\text{OH}}$  absorption from the open N⋯HO—H complex at 3463 cm<sup>-1</sup> and a broader  $\nu^b_{\text{OH}}$  absorption from the closed C=O⋯H—O⋯H—N complex centered at 3455 cm<sup>-1</sup>. It will be argued in the Discussion section that observation of a free  $\nu_{\text{C=O}}$  mode after annealing the matrix is rather impossible in view of the water-assisted tautomeric interconversion. The free  $\nu_{\text{C=O}}$  mode of 2OPM located around 1720 cm<sup>-1</sup> is shifted by about 40 cm<sup>-1</sup> in the complex and appears at 1679 cm<sup>-1</sup>. This shift is well predicted by the *ab initio* calculations summarized in Table 8. No bands characteristic to an open C=O⋯H—O—H complex are identified, and this can be understood in view of the origin of the oxo tautomer as resulting from the proton-transfer reaction converting the hydroxy to the oxo tautomer and operating in the closed H-bonded complex (see further discussion). The results shown in Tables 7 and 8 allow us to conclude that the predicted shifts of the main modes of the two different closed complexes agree rather well with the experimental findings.

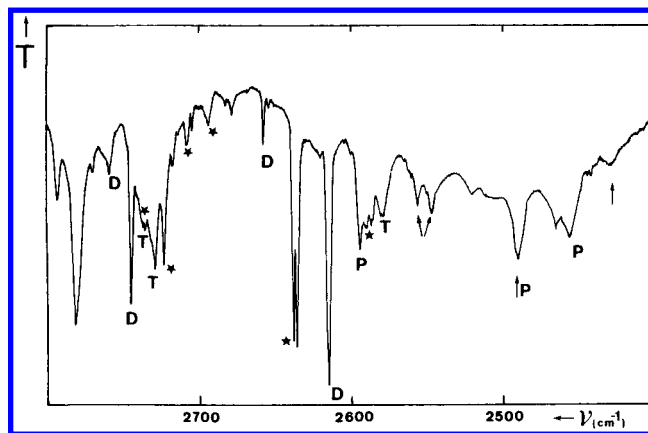


**Figure 5.** FT-IR spectrum (2800–2400 cm<sup>-1</sup>) of 2-hydroxypyrimidine/D<sub>2</sub>O/Ar. D<sub>2</sub>O/Ar 1/200, annealed; ↑ = complex absorptions: D, T, P = dimer, trimer, polymer bands.

**2HPM/D<sub>2</sub>O/Ar.** Additional arguments supporting the conclusions of the spectral analysis presented above was obtained from isotopic D<sub>2</sub>O matrix-doping experiments. Figure 5 illustrates the  $\nu_{\text{OD}}$  frequency region (2800–2400 cm<sup>-1</sup>) of the FT-IR spectrum of a 2HPM/D<sub>2</sub>O/Ar sample at relatively high D<sub>2</sub>O concentration. The sharp bands observed between 2795 and 2580 cm<sup>-1</sup> are all due to the D<sub>2</sub>O monomer (M), dimer (D), and trimer (T) modes,<sup>44</sup> except for a few bands due to the HOD species. The latter are formed by isotopic exchange in the glass vacuum line during preparation of the gaseous D<sub>2</sub>O/Ar mixture and in the 2HPM/2OPM tautomeric interconversion.

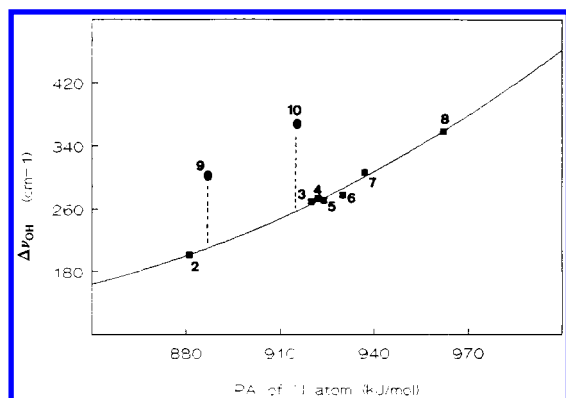
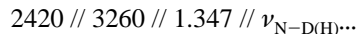
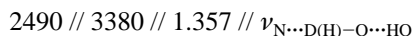
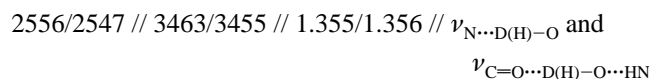


**Figure 6.** Correlation between the (corrected) frequency shift of the bonded water mode  $\nu_{\text{OH}}^{\text{b}}$  and the proton affinity value of the N atom in 1:1 H-bonded complexes  $\text{N} \cdots \text{HO}-\text{H}$ . 2 = pyrimidine;<sup>1</sup> 3 = 3-OH-pyridine;<sup>3</sup> 4 = benzimidazole;<sup>57</sup> 5 = pyridine;<sup>1</sup> 6 = imidazole;<sup>7</sup> 7 = 4-OH-pyridine;<sup>3</sup> 8 = 4-NH<sub>2</sub>-pyridine;<sup>2</sup> 9 and 10 = closed complexes with 2-OH-pyrimidine (this work) and with 2-OH-pyridine,<sup>21</sup> respectively.

The 2570–2400  $\text{cm}^{-1}$  region exhibits  $\text{D}_2\text{O}$ –polymer (P)<sup>44</sup> and complex ( $\text{D}_2\text{O}$  with 2HPM) absorptions, and the latter may be correlated with the  $\text{H}_2\text{O}$  analogs as indicated in the following correlation scheme of  $\nu_{\text{X}-\text{D}}/\nu_{\text{X}-\text{H}}/\text{ISR}$ /vibrational mode data, where the isotopic ratio (ISR) is defined as  $\nu_{\text{X}-\text{H}}/\nu_{\text{X}-\text{D}}$ :



Furthermore, the relative intensities of the different complex bands are largely similar to those in the spectrum of 2HPM/ $\text{H}_2\text{O}/\text{Ar}$ . The observation of the complex  $\nu_{\text{N}-\text{D} \cdots}$  mode is an additional, important proof of the  $\text{D}_2\text{O}$ -assisted tautomeric interconversion of the  $\text{N} \cdots \text{D}-\text{O} \cdots \text{H}-\text{O}-\text{C}$  complex to the  $\text{N}-\text{D} \cdots \text{O}-\text{H} \cdots \text{O}=\text{C}$  complex of the oxo tautomer.

## Discussion

**Open and Closed H-Bonded Base· $\text{H}_2\text{O}$  Complexes in the Vibration Correlation Diagram.** Pimentel and Ault introduced the so-called vibration correlation diagram for H-bonded and proton-transfer base·HX complexes by considering the frequency shifts of the HX stretching mode as a function of the difference of the proton affinity ( $\Delta\text{PA}$ ) value for the base and its acid anion.<sup>45</sup> This concept has been applied by some of us to a series of H-bonded complexes of different bases with water.<sup>46</sup> The vibration correlation diagram involves the correlation between the frequency shift of the bonded-water stretching vibration ( $\nu_{\text{OH}}^{\text{b}}$ ) and the  $\text{PA}_{\text{B}}$  value of the base. Different correlations were observed for different H-bond centers ( $\pi$ , O, N). The difference originates from a different degree of the charge transfer for different basic atoms and different sizes of their lone pairs.<sup>47</sup> If the corrected frequency shift  $\Delta\nu_{\text{OH}}^{\text{b}}$  of H-bonded water for a series of matrix-isolated complexes,  $\text{N} \cdots \text{H}-\text{OH}$  or  $\text{C}=\text{O} \cdots \text{H}-\text{OH}$ , is plotted as a function of  $\text{PA}_{\text{N}}$  and  $\text{PA}_{\text{C}=\text{O}}$  the points representing the closed H-bonded systems,  $\text{N} \cdots \text{H}-\text{O} \cdots \text{HO}$  and  $\text{C}=\text{O} \cdots \text{H}-\text{O} \cdots \text{H}-\text{N}$ , exhibit rather large deviation from the correlation curve for the open  $\text{N} \cdots \text{H}-\text{OH}$  and  $\text{C}=\text{O} \cdots \text{H}-\text{OH}$  complexes. This is illustrated in Figure 6. The deviation, which is caused by a larger frequency shift than

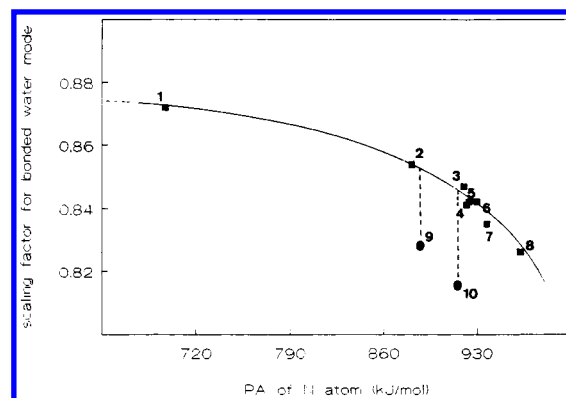


**Figure 7.** Correlation between the optimal scaling factor for the bonded water mode  $\nu_{\text{OH}}^{\text{b}}$  and the proton affinity value of the N(O) atom in 1:1 H-bonded complexes  $\text{N}(\text{O}) \cdots \text{HO}-\text{H}$ . 1 =  $(\text{H}_2\text{O})_2$ ; 2–10 same as in Figure 6.

expected from the  $\text{PA}_{\text{N}}$  value due to cooperativity between the two H bonds in the closed complex, can be taken as a further supporting argument for the assignment of the  $\nu_{\text{OH}}^{\text{b}}$  absorption to the closed complex.

**Optimal Scaling Factors for the  $\nu_{\text{OH}}^{\text{b}}$  Mode in Closed H-Bonded Complexes.** In the previous papers of this series, we have demonstrated that the “optimal” scaling factor,  $\nu^{\text{exp}}/\nu^{\text{th}}$  (this factor, multiplied by the theoretical frequency, gives the experimental frequency), for the bonded water mode  $\nu_{\text{O}}^{\text{b}}$  can be correlated with the proton affinity of the base atom,  $\text{PA}_{\text{B}}$ , which is H-bonded to water.<sup>1–5</sup> The systematic decrease of the optimal scaling factor with increasing  $\text{PA}_{\text{B}}$  value originates from increase of the anharmonicity of the H-bonded OH stretching mode with increasing H-bond strength. Since the *ab initio* frequency calculations in this work were performed in the harmonic approximation, they have to be scaled to correct for the anharmonicity. It can be anticipated that the relatively strong closed H bonds should exhibit larger anharmonicity leading to a smaller value of the scaling factor than in the case of the open complexes with weaker interaction. This is indeed what one observes in the correlation between the optimal scaling factor and  $\text{PA}_{\text{B}}$  as illustrated in Figure 7 for complexes of the  $\text{N} \cdots \text{HO}(\cdots \text{HO})$  type. This figure clearly shows the difference between the closed and open complexes in their spectral appearance. A manifestation of this in Figure 7 is that the point representing the closed water H-bonded complex of 2HPM deviates from the correlation curve for the  $\text{N} \cdots \text{HO}-\text{H}$  open complexes. A similar observation was made before for the closed H-bonded structure of 2-hydroxypyridine with water.<sup>21</sup>

**Reduced Cooperativity between the H Bonds in Closed H-Bonded Complexes.** The H-bond cooperativity effect occurs in systems where there are two or more H bonds and they involve the same or closely neighboring proton-donor or proton-acceptor sites.<sup>48</sup> The cooperativity between the H bonds can be either positive (H-bond strengthening) or negative (H-bond weakening). The effect depends on whether the H-bond sites and the interactions involved are of the same (donor–donor or acceptor–acceptor) type or of the opposite (donor–acceptor) type. In the case of the closed complexes of water with 2HPM and 2OM, a positive cooperativity effect is expected since the same water molecule acts simultaneously as a proton donor and a proton acceptor, and the two H-bond interactions are of the opposite type. A suitable method to evaluate H-bond cooperativity in open linear trimers  $(\text{HA})_3$ , and higher multimers  $(\text{HA})_x$ , is to compare the frequency shifts,  $\Delta\nu_{\text{OH}}$  for the bridged AH bonds with the frequency shift of the AH bond stretch in the open dimer,  $\text{AH} \cdots \text{AH}$ .<sup>49</sup> Due to the experimental observation

of the  $\nu^b_{\text{OH}}$  modes for the open  $\text{N}\cdots\text{HO}-\text{H}$  complex of 2HPM, as well as for the closed  $\text{N}\cdots\text{HO}\cdots\text{HO}$  complexes, it was possible to evaluate the cooperativity factor,  $A_b$ , for the bridged OH bond in the closed complex from the  $\Delta\nu^b_{\text{OH}}(\text{N}\cdots\text{H}-\text{O}\cdots\text{H}-\text{O})/\Delta\nu^b_{\text{OH}}(\text{N}\cdots\text{HO}-\text{H})$  ratio. The value of  $302/207 = 1.46$  was obtained. This value indicates a substantial cooperativity effect, since for linear  $1:2 \text{ B}\cdots\text{H}-\text{O}\cdots\text{HO}$  water complexes the average ratio was 1.37.<sup>49</sup> On the other hand, for the cyclic water trimer ( $\text{H}_2\text{O}$ )<sub>3</sub>, a much larger value of 1.73 was found,<sup>49</sup> which was explained by a mutual fortification of the extra H bond which closes the system to form the cyclic trimer. In the closed H-bonded systems such as those studied in this work, geometrical constraints reduce the H-bond cooperativity. The situation is different when the two H bonds occur in a more ideal, "almost linear" configuration. We illustrated this point in our previous studies where we compared the closed  $\text{N}\cdots\text{H}-\text{O}\cdots\text{HO}$  complex of 2HPM·H<sub>2</sub>O with the open  $\text{N}\cdots\text{HO}-\text{H}$  and  $\text{HO}\cdots\text{H}-\text{O}$  water complexes of 4-NH<sub>2</sub>-pyridine<sup>3</sup> and 4-OH-pyridine,<sup>3</sup> respectively.

**A Double Proton-Transfer Mechanism in the Ground State.** It is clear from the spectral results presented above that the tautomeric equilibrium of the 2HPM/2OPM system is shifted toward the oxo form in the presence of water, but the effect is only clear after the matrix is annealed. This indicates that water assists in the tautomeric interconversion and that this interconversion takes place below 40 K which is the upper limit of the annealing temperature. The process of matrix annealing, which is usually performed for about 15 min, very likely produces the most stable closed 2HPM·H<sub>2</sub>O complex. Though, as we mentioned before, the water-to-base ratio of 1:1 to 5:1 was used which should ensure formation of an excess amount of the 1:1 complex, some amounts of complexes with a higher water content could also be formed in the annealing process. In this complex, the protomeric reaction takes place. There have been several theoretical and experimental studies, which we will now review, that provide some explanation regarding the possible mechanism of this reaction.

The first piece of evidence is provided by *ab initio* calculations of the barrier height for the protomeric reaction with and without a water molecule. Several authors reported *ab initio* calculated barrier heights for proton transfer in the isolated tautomers of 2-hydroxypyridine and these vary between 190 and 140 kJ/mol.<sup>15,20</sup> The barrier height decreases drastically to about 50 kJ/mol when water is H-bonded to 2-hydroxypyridine, allowing for a concerted mechanism with a double proton jump to operate.<sup>20</sup> A similar barrier height of 48.2 kJ/mol (MP2/DZ95\*\* result) was found in *ab initio* calculations for the intermolecular double proton transfer process of 2HPM complexed with one water molecule.<sup>26,27</sup> It is possible that if more water molecules are involved, the barrier lowers even more. The barrier heights for proton transfer between the isolated hydroxy and oxo tautomers indicate that proton movement cannot effectively occur at 40 K. However, the lowering of the barrier by water may enable the transfer.

Secondly, *ab initio* calculations on the lowest excited states of the 2HPM-water complexes<sup>26</sup> indicated that a possible route for the tautomeric interconversion may involve electronic excitation of the complex. The barrier height of only 18.3 kJ/mol was found in CASPT2/DZ95\*\* calculations of the first electronically excited state,  $S_1$  ( $^1\pi\pi^*$ ). The calculations also predicted that the reaction should be strongly exothermic by about 64.6 kJ/mol. In the experiment performed in this work, the matrix sample remained inside the cryostat positioned in the FT-IR instrument, so that the sample can only absorb energy

either from the IR (Globar) source or from the interferometer laser. It is therefore unlikely that an electronic excitation is involved in the process.

A possible explanation of a double proton transfer in the tautomerization process of the 2HPM/2OPM/H<sub>2</sub>O system can be proton tunneling. Recently, Hammes-Schiffer and Tully have demonstrated using the molecular dynamics quantum transition (MDQT) method that proton transfer in the phenol-amine complex in methyl chloride solution is enhanced in vibrationally excited levels.<sup>24,56</sup> Since the MDQT method treats H and D atoms quantum mechanically, the proton-transfer reaction can occur below the barrier through quantum tunneling. Furthermore, it is a faster process than the vibrational relaxation.<sup>24,51</sup> Such a tunneling may take place in the 2HPM/2OPM water-assisted tautomeric interconversion. There are other examples of proton tunneling assisted by solvent. A ground-state reverse proton transfer (GSRPT) was found in 7-hydroxyquinoline catalyzed by methanol in studies of Chou and Martinez.<sup>52,53</sup> These experiments provided support for a two-step mechanism of the GSRPT in 7-hydroxyquinoline proposed by Konijnenberg *et al.*;<sup>54</sup> the first step involving thermally-induced fluctuations into a well-defined conformation suitable for the proton-transfer process and the second step involving the tunneling. The mechanism can be similar in the proton-transfer process observed in the present work for 2HPM and 5B2HPM. Since the GSRPT process in 7-hydroxyquinoline occurs at room temperature and the first solvation shell around the solute molecule involves two solvent molecules, the process is accompanied by a large entropy decrease and a rather small decrease in enthalpy resulting in a large, positive free enthalpy change.<sup>52</sup> In a low-temperature matrix, the structural reorganization is probably not as significant in terms of free enthalpy, since the low-temperature favors the enthalpy-decreasing formation of the closed complex, and the effect of the negative entropy change is strongly reduced.<sup>55</sup> However, it may still be sufficient to drive the reaction forward.

## Summary

The FT-IR matrix-isolation technique and *ab-initio* theoretical calculations have been used to study the H-bonding interaction of water with 2-hydroxypyrimidine and its 5-bromo derivative. Both compounds occur predominantly in the hydroxy tautomeric forms in Ar matrices, and the experimentally estimated values for the hydroxy/oxo equilibrium constants,  $K_T(\text{h/o})$ , are 60 and 184, respectively. Interpretation of the IR spectra of the complexes with water assisted by *ab initio* calculated energies, frequencies, and intensities indicates the presence of the closed H-bonded  $\text{N}\cdots\text{H}-\text{O}\cdots\text{H}-\text{O}$  complex of the hydroxy tautomer in the early stages of the experiment, but matrix annealing induces an increasing presence of the closed  $\text{C}=\text{O}\cdots\text{H}-\text{O}\cdots\text{H}-\text{N}$  complex of the oxo tautomer. An *ab initio* assisted assignment of the main bands of the two complexes is presented. We demonstrated with the use of the earlier established relations that a relatively strong cooperativity exists between the two H bonds in the closed complexes. An analysis of the characteristics of the experimentally observed hydroxy  $\rightarrow$  oxo tautomerism in water-doped matrices suggests that the mechanism of the proton transfer involves proton tunneling. However, on the basis of the results of the present study, we could not definitely determine whether the proton transfer takes place in the 1:1 closed 2HPM·H<sub>2</sub>O complex or it involves complexes with higher water content.

**Acknowledgment.** This work was part of the ECC research project ERB CIPA-CT93-0108, and cooperation between the



groups of Leuven and Tucson was supported by the NATO International Collaborative Grant INT-9313268. G.M. acknowledges the Belgian NFWO for a permanent Research Fellowship. J.S. acknowledges the support of the Belgian IWONL. L.A. and J.S. acknowledge the support from the Office of Health and Environmental Research, Office of Energy Research and the Department of Energy (Grant No. DEFG0393ER61605).

**Supporting Information Available:** Table of predicted geometry parameters of 2-hydroxypyrimidine and its  $N_1 \cdots H-O \cdots H-O_{10}$  H-bonded complex with water, and of 2-pyrimidone and its  $C_2=O \cdots H-O \cdots H-N_1$  H-bonded complex with water (1 page). Ordering information is given on any current masthead page.

## References and Notes

- (1) Destexhe, A.; Smets, J.; Adamowicz, L.; Maes, G. *J. Phys. Chem.* **1994**, *98*, 1506.
- (2) Smets, J.; Adamowicz, L.; Maes, G. *J. Phys. Chem.* **1995**, *99*, 6387.
- (3) Buyl, F.; Smets, J.; Maes, G.; Adamowicz, L. *J. Phys. Chem.* **1995**, *99*, 14967.
- (4) Smets, J.; Destexhe, A.; Adamowicz, L.; Maes, G. *J. Phys. Chem.* **1997**, *101*, 6583.
- (5) Smets, J.; Maes, G.; Adamowicz, L. *J. Phys. Chem.* **1996**, *101*, 6434.
- (6) Nowak, M. J.; Szczepaniak, K.; Barski, A.; Shugar, D. *J. Mol. Struct.* **1980**, *62*, 47. Czerninski, R.; Kuczera, K.; Rostkowska, H.; Nowak, M. J.; Szczepaniak, K. *J. Mol. Struct.* **1986**, *140*, 235. Radchenko, E. D.; Plokhotnichenko, A. M.; Sheina, G. G.; Blagoi, Yu. P. *Biofizika* **1989**, *28*, 559. Lapinski, L.; Czerninski, R.; Nowak, M. J.; Fulara, J. *J. Mol. Struct.* **1990**, *220*, 147.
- (7) Smets, J.; Maes, G. *Chem. Phys. Lett.* **1991**, *187*, 532.
- (8) Nowak, M. J.; Lapinski, L.; Fulara, J.; Les, A.; Adamowicz, L. *J. Phys. Chem.* **1992**, *96*, 1562.
- (9) Lapinski, L.; Fulara, J.; Nowak, M. J. *Spectrochim. Acta* **1990**, *46A*, 61.
- (10) Szczesniak, M.; Kwiatkowski, J. S.; KuBulat, K.; Szczepaniak, K.; Person, W. B. *J. Am. Chem. Soc.* **1988**, *110*, 8319.
- (11) Lapinski, L.; Nowak, M. J.; Fulara, J.; Les, A.; Adamowicz, L. *J. Phys. Chem.* **1990**, *94*, 6555.
- (12) Vrancken, H.; Smets, J.; Maes, G.; Lapinski, L.; Nowak, M. J.; Adamowicz, L. *Spectrochim. Acta A* **1994**, *50*, 875.
- (13) Smets, J.; Maes, G.; Adamowicz, L., manuscript in preparation.
- (14) Beak, P.; Covington, J. B.; Smith, S. G.; White, J. M.; Ziegler, J. M. *J. Org. Chem.* **1980**, *45*, 1354.
- (15) Field, M. J.; Hillier, J. H. *J. Chem. Soc., Perkin Trans. 2* **1987**, 617.
- (16) Held, A.; Pratt, D. W. *J. Am. Chem. Soc.* **1993**, *115*, 9708.
- (17) Favero, S.; Hatherley, L. D.; Brown, R. D.; Goddfrey, P. D.; Pierlot, A. P.; Canlinatti, W.; Damiani, D.; Melandri, B. *J. Phys. Chem.* **1993**, *97*, 46.
- (18) Szafran, M.; Karelson, M. M.; Katritzky, A. R.; Koput, J.; Zerner, M. C. *J. Comput. Chem.* **1993**, *14*, 371.
- (19) Del Belie, J. E. *J. Phys. Chem.* **1994**, *98*, 5902.
- (20) Barone, V.; Adamo, C. *J. Phys. Chem.* **1995**, *99*, 15062.
- (21) Smets, J.; Vrancken, H.; Adamowicz, L.; Maes, G., manuscript in preparation.
- (22) Vener, M. V.; Scheiner, S. *J. Phys. Chem.* **1995**, *99*, 642.
- (23) Luth, K.; Scheiner, S. *J. Phys. Chem.* **1995**, *99*, 7352.
- (24) Hammes-Schiffer, S.; Tully, J. C. *J. Phys. Chem.* **1995**, *99*, 5793.
- (25) Kasha, M.; Heldt, J.; Gormin, D. *J. Phys. Chem.* **1995**, *99*, 7281.
- (26) Sobolewski, A. L.; Domcke, W. In *The Reaction Path in Chemistry: Current Approaches and Perspectives, Ab-initio studies of Reaction Paths in Excited-State Hydrogen-Transfer Processes*; Mezey, P. G., Ed.; Kluwer Academic Publishers: New York, 1995; pp 257–282.
- (27) Sobolewski, A. L.; Adamowicz, L. *J. Phys. Chem.* **1995**, *99*, 14277.
- (28) Forberg, S.; Solbakk, J. *Acta Chem. Scand.* **1970**, *24*, 3230.
- (29) Beak, P.; Fry, F. S.; Lee, J.; Steele, F. *J. Am. Chem. Soc.* **1976**, *98*, 171.
- (30) Person, W. B.; Szczepaniak, K.; Szczesniak, M.; Kwiatkowski, J. S.; Hernandez, L.; Czerninski, R. *J. Mol. Struct.* **1989**, *194*, 239.
- (31) Maes, G. *Bull. Soc. Chim. Belg.* **1981**, *90*, 1093.
- (32) Graindourze, M.; Smets, J.; Zeegers-Huyskens, Th.; Maes, G. *J. Mol. Struct.* **1990**, *222*, 345.
- (33) Hunt, R. R.; McOmie, J. F.; Sayer, E. R. *J. Chem. Soc.* **1959**, 525.
- (34) Wheeler, K. *J. Am. Chem. Soc.* **1909**, *42*, 301.
- (35) Schafer, A.; Horn, H.; Ahlrichs, R. *J. Chem. Phys.* **1992**, *97*, 2571.
- (36) *Gaussian Basis Sets for Molecular Calculations*; Huzinaga, S., Ed.; Elsevier: New York, 1984.
- (37) Gaussian 92; Frisch, C. P. M. J.; Trucks, G. W.; Head-Gordon, M.; Gil, P. M. W.; Wong, W. M.; Foresman, J. B.; Johnson, B. G.; Schlegel, H. B.; Robb, M. A.; Replogie, E. S.; Gomperts, R.; Andres, J. L.; Raghavachari, K.; Binkley, J. S.; Gonzales, C.; Martin, R. L.; Fox, D. J.; Defrees, D. J.; Baker, J.; Stewart, J. J. P.; Pople, J. A. Gaussian Inc.: Pittsburgh, PA, 1992.
- (38) Jaworski, A.; Szczepaniak, M.; Szczepaniak, K.; Kubulat, K.; Person, W. B. *J. Mol. Struct.* **1990**, *223*, 63.
- (39) Person, W. B.; Szczepaniak, K. *Vibrational Spectra and Structure*; Durig, J. R., Ed.; Elsevier: Amsterdam, 1993.
- (40) Schoone, K.; Houben, L.; Smets, J.; Adamowicz, L.; Maes, G. *Spectrochim. Acta A*, in press.
- (41) Lias, S. G.; Liebman, J. F.; Levin, R. D. *J. Phys. Chem. Ref. Data* **1984**, *13*, 695.
- (42) Katritzky, A. R.; Szafran, M.; Stevens, J. *J. Mol. Structure (THEOCHEM)* **1989**, *184*, 179.
- (43) Engdahl, A.; Nelander, B. *J. Mol. Struct.* **1989**, *193*, 101.
- (44) Bentwood, R. M.; Barnes, A. J.; Orville-Thomas, W. J. *J. Mol. Spectrosc.* **1980**, *84*, 381.
- (45) Ault, B. S.; Pimentel, G. C. *J. Phys. Chem.* **1975**, *79*, 615.
- (46) Maes, G.; Smets, J. *J. Mol. Struct.* **1992**, *270*, 141.
- (47) Allen, L. C. *J. Am. Chem. Soc.* **1975**, *97*, 6921.
- (48) Huyskens, P. L. *J. Am. Chem. Soc.* **1977**, *99*, 2578.
- (49) Maes, G.; Smets, J. *J. Phys. Chem.* **1993**, *97*, 1818.
- (50) Leś, A.; Adamowicz, L.; Nowak, M. J.; Lapinski, L. *J. Mol. Struct (THEOCHEM)* **1992**, *277*, 313.
- (51) Hammes-Schiffer, S.; Tully, J. C. *J. Chem. Phys.* **1994**, *101*, 4567.
- (52) Chou, P.; Martinez, S. S. *Chem. Phys. Lett.* **1995**, *235*, 463.
- (53) Lavin, A.; Collins, S. *Chem. Phys. Lett.* **1993**, *207*, 514.
- (54) Konijnenberg, J.; Ekelmans, G. B.; Huizer, A. H.; Varma, A. G. *O. J. Chem. Soc., Faraday Trans. II* **1989**, *85*, 39.
- (55) Maes, G. In *Low Temperature Molecular Spectroscopy*; NATO ASI; Fausto, R., Ed.; Kluwer Academic Press: New York, in press.
- (56) Maes, G.; Smets, J.; Adamowicz, L.; McCarthy, W.; Van Bael, M. K.; Houben, L.; Schoone, K. *J. Mol. Struct.* **1997**, *315*, 410.